

Evidence for vortex surface pinning in $\text{YBa}_2\text{Cu}_3\text{O}_{7-\delta}$ from the frequency dependence of the complex penetration depth

Alain Pautrat, Christophe Goupil, and Charles Simon

Laboratoire CRISMAT, UMR 6508 du CNRS et de l'Institut Supérieur de la Matière et du Rayonnement, 14050 CAEN, France

Norbert Lütke-Entrup, Bernard Plaçais, Patrice Mathieu, and Yvan Simon

Laboratoire de Physique de la Matière Condensée de l'École Normale Supérieure, UMR 8551 du CNRS, associée aux universités Paris 6 et 7, 24 rue Lhomond, F-75231 Paris Cedex 5, France

Alexander Rykov and Setsuko Tajima

Superconductivity Research Laboratory, ISTEC, Tokyo 135, Japan

(Received 26 July 2000; published 3 January 2001)

We have measured the high-frequency complex skin depth in the mixed state of a large untwinned YBaCuO crystal. Our frequency range (0.1–3 MHz) covers the pinning crossover in the vicinity of the first-order transition ($T=85\text{--}87$ K). The spectrum deviates from that expected from bulk-pinning theories but closely follows that predicted by a surface pinning model which is based on two-mode electrodynamics, free bulk vortex flow and surface slippage conditions. Above the first-order line, critical currents vanish and the ideal pinning-free response is recovered. This experiment points out the irrelevance of pinning by point defects in clean YBaCuO , and adds a piece to the physics of the first-order transition in high- T_c materials.

DOI: 10.1103/PhysRevB.63.054503

PACS number(s): 74.72.Bk, 74.60.Ge, 74.25.Nf

The nature of vortex pinning in clean high- T_c materials is still the subject of an intense debate, although some consensus seems to appear in favor of a bulk scenario with many pinning centers.¹ The theoretical problem is that of the weak pinning of an elastic medium by disorder; it includes many systems similar to the contact line of a liquid meniscus,² charge density waves,³ or superfluid vortex arrays.⁴ In this respect, untwinned YBaCuO crystals has often been proposed as a model system,⁵ since pinning is believed to be due to oxygen vacancies acting as point defects. Our purpose is to check this assumption experimentally, by relying on the high-frequency vortex response.

The frequency dependence of the ac response has been long recognized,^{6,7} and recently demonstrated on low- T_c materials,⁸ to be a powerful tool for the investigation of the pinning mechanism in the vortex state. As a matter of fact, the universal shape of frequency spectrum is not concerned with the temperature or magnetic field dependencies of thermodynamic parameters, which generally obscure the dynamical aspects of the ac response. Few experiments were previously done in YBaCuO by this technique using heavily twinned thin films or crystals.^{9–11} In our opinion, extended defects and size effects make their analysis very intricate. Moreover, strong discrepancies appear when one compares experimental results and theoretical predictions for bulk pinning.⁹ We propose here to use a large good quality untwinned crystal allowing a direct comparison between pinning theories and the experiment.

In order to understand why it is really necessary to study a large crystal, let us precise the predictions of prevalent ac models, which fall into two categories. The first one, introduced by Gittleman and Rosenblum and Campbell (GRC model), describes the frequency response in the presence of bulk pinning^{6,7} by a local elastic interaction with the host crystal, characterized by a return spring constant α_L .^{6,7} The

second category includes the two-mode (TM) model, introduced by Sonin¹² and four of us;^{8,13} it is well suited for the study of pinning by surfaces or interfaces. Predictions can be put to test by using the simple geometry of a superconducting half space ($z \leq 0$) in normal field $\mathbf{B} = B\hat{z}$. In the case of an anisotropic material the surface should be parallel to one of the crystal facets. A small transverse field $b_x = be^{-i2\pi ft}$ is used to excite small linear oscillations $\delta\omega_x = Bu(z)e^{-i2\pi ft}$ of the vortex field $\boldsymbol{\omega}$ [displacement $u(z)$, tilt $v = du/dz$] about the equilibrium position ($\boldsymbol{\omega} = B\hat{z}$ in average). Disregarding acceleration terms which are beyond current resolution, the vortex displacement at the surface $u(0)$ can be deduced from electric field $E_y(0)$ using the Josephson relation $E_y \approx B\dot{u}$. Then, with Maxwell equations, one can rewrite the apparent complex penetration depth in the form

$$\lambda_{ac} = E_y / (-i2\pi f b) = Bu(0) / \mu_0 K, \quad (1)$$

where $K = b / \mu_0$ is the integrated current density over the half-space.

Bulk-pinning models involve a local force equation [linear stiffness JB/u or complex conductivity $\sigma_{ac} = JB / (-i2\pi fu)$], with a single length-scale, $1/ik_{\text{bulk}} = \lambda_{ac}$, that rules the decay of fields and currents J in the bulk (one-mode electrodynamics). As a matter of fact, with $K = J(0)\lambda_{ac}$ in Eq. (1), one obtains $\lambda_{ac}^{-2} = \mu_0 JB/u$, which is nothing but the definition of the complex skin depth in an Ohmic medium. In the GRC model, the mere addition of a linear restoring force density $-\alpha_L u$ to the viscous drag term leads to the popular expression

$$\frac{1}{\lambda_{ac}^2} = \frac{1}{\lambda_C^2} - \frac{2i}{\delta_f^2} \quad (\text{bulk}), \quad (2)$$

where $\delta_f = (\rho_f / \mu_0 \pi f)^{-1/2}$ is the flux-flow skin depth and $\lambda_C = B / \sqrt{\mu_0 \alpha_L}$ the Campbell length. In the absence of pinning ($\alpha_L = 0$) the ac response $\lambda_{ac} = (1+i)\delta_f/2$ is similar to that of an ordinary metal. As suggested in Refs. 14,15 the Labusch coefficient α_L should be frequency dependent at finite temperature, in the form $\alpha_L(T) = \alpha_{L0} i 2 \pi f / (1 + i 2 \pi f \tau)$, where $\tau(T)$ is a characteristic vortex thermal-creep time; but this would result in a low frequency divergence, which is not observed experimentally.^{7,9} Likewise, are the $\log f$ corrections in λ_C^2 predicted in the two-level model of Koshelev and Vinokur for a glassy vortex creep.^{16,17} Except for these low-frequency peculiarities, bulk scenarios have in common a sharp pinning-frequency crossover similar to that in Eq. (2), with a two decades frequency-width as seen in Fig. 2.

In contrast, pinning by surface irregularities entails a non-local treatment, since superficial tensile strains are compensated by bulk currents. The penetration depth $\lambda_V = \lambda \sqrt{\mu_0 \varepsilon / \omega}$ of these currents has been calculated in the phenomenological theory of Mathieu and Simon, where $\varepsilon \varphi_0$ is the line tension.¹⁸ The nearly uniaxial anisotropy of YBaCuO crystals, can be taken into account by replacing everywhere ε by ε / γ^2 for a \hat{c} -oriented facet, and $\varepsilon \gamma^2$ for facets that are parallel to \hat{c} .¹⁹ However, since $\lambda_V \ll \lambda$ is small, currents can still be regarded as quasisuperficial, with a surface density $K_S = -\varepsilon_x(0)$.¹⁸ As pointed out in Refs. 8,12,13, these currents play an important role in the ac response as a second mode in parallel to the flux-flow mode [penetration depth $1/ik_f$, current $K_f = ik_f B u(0) / \mu_0$]. Its relative amplitude is ruled by a surface condition $u(0) + l v(0) = 0$, which introduces a new phenomenological length $l(\omega, T)$ characteristic of the surface pinning strength: $l = 0$ for strong pinning and $l = \infty$ for ideal surface conditions. Putting $K = K_f + K_S$ in Eq. (1), one obtains, with $\varepsilon_x(0) = \varepsilon v(0)$ in the above boundary condition

$$\frac{1}{\lambda_{ac}} = \frac{\mu_0(K_S + K_f)}{B u(0)} = \frac{1}{L_S} + \frac{1-i}{\delta_f} \quad (\text{surface}). \quad (3)$$

The surface contribution appears as an additive term $1/L_S = \mu_0 \varepsilon / \omega l$, in the surface admittance (or $1/\lambda_{ac}$). It should be stressed that, unlike the Campbell length λ_C , L_S , in a two mode model, is not a true quasistatic penetration depth.⁸

As seen in the graphs of Fig. 2 [full line for Eq. (3) and dashed line for Eq. (2)], a striking difference appears between the two predictions, irrespective of any quantitative analyze; whereas the crossover width is of two frequency decades in the bulk scenario, it extends over *four decades* in the two-mode model. This leads us to the following remarks. (i) One cannot rely on experiments done in the quasistatic regime to decide about the nature of pinning and distinguish between surface and bulk mechanisms. This is meant for most of ac experiments, including the Hall-probe array technique,²⁰ which otherwise is very powerful for the study of edge-effects. (ii) The transition can be considerably affected by the sample geometry. Indeed, if one keeps in mind that Eq. (3) implies the full development of a free-flow half-space response in the bulk, any interference between op-

posed faces will result in a narrowing of the crossover. This size effect, which is against intuition, has been clearly demonstrated in low T_c 's,⁸ whenever the sample thickness L becomes comparable to the largest penetration depth, i.e., δ_f . In this case Eq. (3) should be replaced by

$$\frac{1}{\lambda_{ac}} = \frac{1}{L_S} + \frac{1-i}{\delta_f} \coth \frac{(1-i)L}{2\delta_f}, \quad (4)$$

which entails a suppression of the low-frequency tail whenever $L \lesssim \delta_f$.

On the other hand, one may expect an extraneous broadening of spectrum (2) in the presence of strong heterogeneity in the bulk-pinning parameter α_L . However simulations show that these inhomogeneities do not affect the crossover width by more than 10% for a broad distribution $\Delta \alpha_L \sim \alpha_L$. We conclude that, under well controlled experimental conditions, a significant and robust contrast exists in the linear ac responses of different pinned states.

The sample is a YBa₂Cu₃O_{7- δ} crystal with the following dimensions: length $l_b = 4.5$ mm, thickness $l_c = 1.17$ mm, width $l_a = L = 0.58$ mm. Details of its preparation are given in previous papers.^{21,22} The sample was annealed at 480 °C for 48 h, so as to reach the slightly overdoped regime with $T_c \approx 92$ K, while avoiding a too large amount of oxygen disorder. Optical inspection reveals a standard roughness. The presence of a reversibility line, coinciding with a first order transition, has been verified in this sample up to more than 7 teslas. Sharp jumps in magnetization using SQUID technique have been observed, and dc transport measurements in the same sample have been published.²²

As sketched in Fig. 1, the dc field ($B \leq 6T$) is orientable in the a - c plane and the ac probe-field ($b_{ac} \leq 1 \mu T$), created by a solenoidal coil (not shown in the figure), was carefully aligned with the \hat{c} axis. At the high frequencies of the experiment, bulk currents, along the b direction, are confined at the main faces $l_b \times l_c$ within a skin layer $\delta_f < l_a$. The experimental response is the flux Φ_{ac} through a ten-turn pick-up coil, which is wound at the midheight of the sample and glued in order to minimize mechanical vibrations. The signal, i.e., the apparent penetration depth in the \hat{a} direction, is defined as $\lambda_{ac} = \lambda' + i\lambda'' = \Phi_{ac} / 2b l_b$. This implies that flux penetration through the \hat{c} -oriented end faces may be neglected; this 1D approximation is well justified if we except a narrow working range when $\mathbf{B} \parallel \hat{c}$ (fields close and smaller than the irreversibility field B^* , and low frequencies). The signal, i.e., its amplitude and phase, was calibrated against

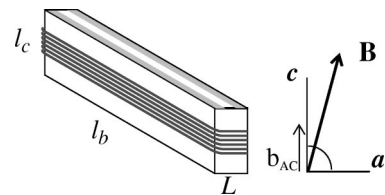


FIG. 1. Sketch of the experimental arrangement showing the crystal and fields orientations, the pick-up, and the 1D geometry of flux penetration (gray area).

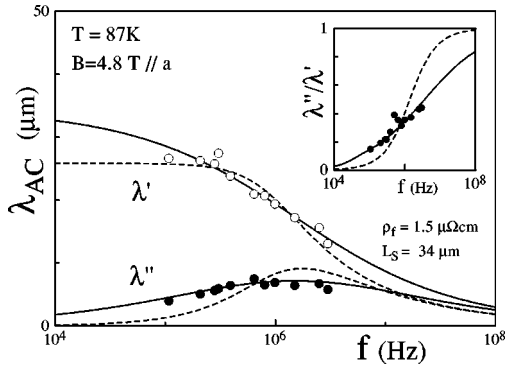


FIG. 2. Frequency dependence of the penetration depth at $T = 87$ K and $B = 4.8$ T, and the theoretical fits to Eq. (3) for surface pinning (full line) and Eq. (2) for bulk pinning (dashed line). In the inset, the tangent of the loss angle ($\tan \varphi = \lambda''/\lambda'$) is plotted as function of frequency so as to illustrate the strong deviations from the bulk-pinning response.

the flux through the gap between the pick-up coil and the sample in the Meissner state. The gap size itself (~ 100 μm) was measured independently by comparing the Meissner signal to the full penetration (low-frequency normal-state response). This normalization procedure yields 1–2 degrees of phase accuracy, and a resolution $\delta\lambda_{ac}\delta\lambda_{ac} \sim 1\text{--}3$ μm . Within this precision, the London penetration length, which does not exceed 0.6 μm in the explored temperature range, as well as the penetration of the surface mode are negligible.

Let us first discuss results in transverse field ($B \parallel \hat{a}$). Figure 2 shows typical spectra measured in this geometry, together with theoretical fits by Eqs. (2) and (3). Obviously Eq. (2) is unable to account for the frequency spectrum $\lambda''(f)$; a fit of the phase, as shown in the inset of Fig. 2, is particularly discriminating. By contrast, the quality of the fits to Eq. (3) gives clear evidence for the surface scenario. Now, in order to estimate a small bulk contribution to pinning, we fit systematically our results by introducing both sources of pinning [see Eq. (1) of Ref. 23], where λ_C and L_S are two adjustable parameters. For data of Fig. 2, for example, we

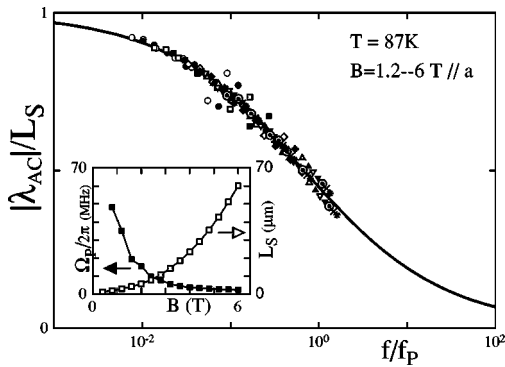


FIG. 3. Frequency dependence of the penetration depth, in reduced units, at $T = 87$ K for fields between 1.2 and 6 T in steps of 0.4 T. The fitted parameters, i.e., $L_S(B)$ and the ‘‘pinning frequency’’ $f_p(B) = f \delta_f^2 / L_S^2$ are shown in the inset. The solid line is graph of $(1 + 2x + 2x^2)^{-0.5}$ from Eq. (3).

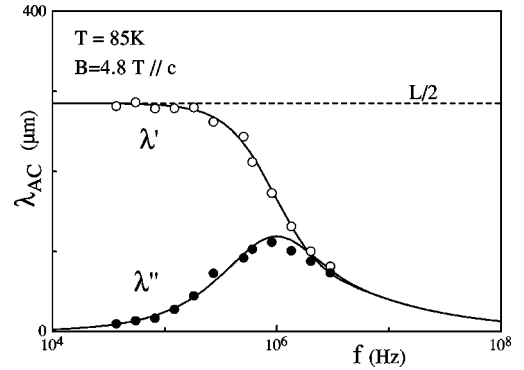


FIG. 4. Typical complex spectrum observed in the so-called ‘‘liquid phase’’ ($B > B^* = 4$ T). The solid line is a fit to Eq. (4) for the ideal response with $\rho_f = 25$ $\mu\Omega\text{cm}$ and $L_S = \infty$.

found $1/L_S = 0.029 \pm 0.002$ μm^{-1} and $1/\lambda_C < 0.005$ μm^{-1} . Over more than 50 recorded spectra, we always found $1/\lambda_C$ to be zero *within experimental accuracy*. Our standard untwinned YBaCuO crystal certainly contains a number of small size or pointlike defects, including oxygen vacancies density fluctuations, so that we are led to the conclusion that such bulk defects do not significantly contribute to vortex pinning.

Data for different magnetic fields ($B \parallel \hat{a}$) have been collected in Fig. 3 and plotted in reduced units so as to point out the relevance of Eq. (3) over the investigated field range. From the field dependence of L_S in Fig. 2, and $\mu_0 \epsilon \gamma^2 = (B_{c2} - B) / 2\kappa_c^2$ with $B_{c2,a} \sim 25$ T and $\kappa_c^2 = \kappa^2 / \gamma^2 \sim 100$, we estimate $l = 0.3\text{--}0.9$ μm , a value of the surface pinning length which is quite standard according to previous measurements in conventional materials.⁸

Unfortunately, the smallness of the penetration length and the correlative large pinning frequencies, preclude the application of our technique to lower temperatures. In contrast, our investigated temperature range (84–87 K) allows us to cross the reversibility line $B^*(T)$ for $B \parallel \hat{c}$. In spite of the

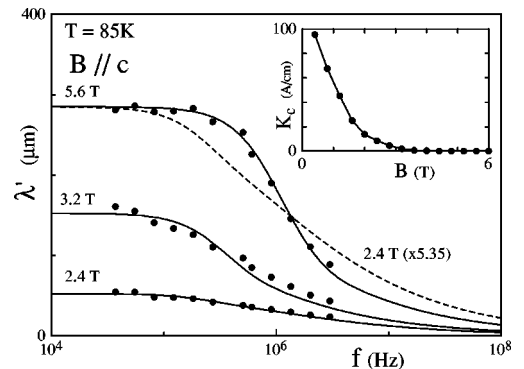


FIG. 5. Frequency dependence of the real part of the penetration depth at $T = 85$ K for $B \parallel \hat{c}$. Fits to Eq. (4) (full lines) yield $L_S = 64$ and 328 μm at 2.4 and 3.2 T in the ‘‘solid phase’’ and $L_S = \infty$ at 5.6 T in the ‘‘liquid phase.’’ The 2.4 T spectrum has been magnified to emphasize changes in the frequency dependence. The inset shows the steep decrease of the pinning strength K_c as defined in the text.

abovementioned restrictions about end effects, we can still draw some important conclusions on this first order transition line, as it is one of the most exciting features of the vortex phase diagram.

The magnetic field being aligned with the \hat{c} axis, the temperature $T=85$ K is chosen so that $B^*\simeq 4T$, as measured in dc transport.²² In this geometry, size effects must be accounted for, due to large values of ρ_f (smaller B_{c2}) making δ_f exceed the sample thickness L at low frequencies. Under these conditions, results must be fitted to Eq. (4) instead of Eq. (3) (eventually including a λ_C term). A typical high-field spectrum ($B>B^*$) is shown in Fig. 4; it displays the ideal normal-like transition from the full penetration ($\lambda'=L/2$) at low frequency to the skin-effect regime ($\lambda'=\lambda''\ll L$). This is confirmed by a fit to Eq. (4), yielding $1/L_S\approx 0$ (and $1/\lambda_C\approx 0$).

In Fig. 5 we have reported $\lambda'(f)$, the real part of λ_{ac} , in the so-called ‘‘solid’’ and ‘‘liquid’’ vortex states. The $B=5.6$ T spectrum above B^* is again fitted by Eq. (4) with $1/L_S\approx 0$. We stress that, only above B^* , $\lambda'(0)=L/2$, as expected from a transparent metal at low frequencies. The

two spectra below B^* exhibit the two-mode-like response. Again, a phase diagram, not shown in Fig. 5, confirms the frequency dependence of a pure surface pinning. The steep decrease of the pinning strength at B^* , expressed in terms of a critical-current density⁸ $K_c=(1/L_S)\sqrt{B\varphi_0/\mu_0^2}$ (A/m), is shown in the inset.

In conclusion, the frequency spectrum of the depinning crossover of an untwinned crystal of YBCO demonstrates that the sources of pinning are localized at the surface, while vortex flow is free in the bulk. This experiment questions the relevance of common interpretations of critical currents and vortex pinning, including the classical weak collective-pinning approach. It also suggests that the interpretation of the first order transition should be reconsidered in light of these results. One may wonder at the vanishing of surface pinning being simultaneous with the bulk first order transition; the paradox is only apparent, since surface pinning also involves the bulk parameters.

This work was partially supported by NEDO, Japan for the R&D of Industrial Science and Technology Frontier Program.

-
- ¹M. Tinkham, *Introduction to Superconductivity*, 2nd ed. (McGraw-Hill, New York, 1996).
- ²P. G. De Gennes, *Rev. Mod. Phys.* **57**, 827 (1985).
- ³G. Grüner, *Rev. Mod. Phys.* **60**, 1129 (1988).
- ⁴E. B. Sonin, *Rev. Mod. Phys.* **59**, 87 (1987).
- ⁵G. Blatter *et al.*, *Rev. Mod. Phys.* **66**, 1125 (1994).
- ⁶J. I. Gittleman and B. Rosenblum, *Phys. Rev. Lett.* **16**, 734 (1966).
- ⁷A. M. Campbell, *J. Phys. C* **2**, 1492 (1969).
- ⁸N. Lütke-Entrup *et al.*, *Phys. Rev. Lett.* **79**, 2538 (1997); *Physica B* **255**, 75 (1998).
- ⁹N. Belk *et al.*, *Phys. Rev. B* **53**, 3459 (1996).
- ¹⁰D. S. Reed *et al.*, *Phys. Rev. B* **49**, 4384 (1994).
- ¹¹J. Kötzler *et al.*, *Phys. Rev. Lett.* **72**, 2081 (1994).
- ¹²E. B. Sonin, A. K. Tagantsev, and K. B. Traito, *Phys. Rev. B* **46**, 5830 (1992).
- ¹³B. Plaçais *et al.*, *Phys. Rev. B* **54**, 13 083 (1996).
- ¹⁴M. W. Coffey and J. R. Clem, *Phys. Rev. Lett.* **67**, 386 (1991); *Phys. Rev. B* **45**, 9872 (1992).
- ¹⁵E. H. Brandt, *Phys. Rev. Lett.* **67**, 2219 (1991).
- ¹⁶A. E. Koshelev and V. M. Vinokur, *Physica C* **173**, 465 (1991).
- ¹⁷C. J. van der Beek, V. B. Geshkenbein, and V. M. Vinokur, *Phys. Rev. B* **48**, 3393 (1993).
- ¹⁸P. Mathieu and Y. Simon, *Europhys. Lett.* **5**, 67 (1988); T. Hocquet, P. Mathieu, and Y. Simon, *Phys. Rev. B* **46**, 1061 (1992).
- ¹⁹Y. Simon, B. Plaçais, and P. Mathieu, *Phys. Rev. B* **50**, 3503 (1994); B. Plaçais, P. Mathieu, and Y. Simon, *Physica C* **235-240**, 3049 (1994).
- ²⁰D. T. Fuchs *et al.*, *Nature (London)* **391**, 373 (1997).
- ²¹A. I. Rykov and S. Tajima, *Advances in Superconductivity VIII*, edited by H. Hayakawa and Y. Enomoto (Springer-Verlag, Tokyo, 1996), p. 341.
- ²²A. Pautrat *et al.*, *Phys. Rev. B* **59**, 199 (1999).
- ²³N. Lütke-Entrup *et al.*, *Physica B* (to be published).